

## IX. PHYSICAL ELECTRONICS AND SURFACE PHYSICS\*

### Academic Research Staff

Prof. R. E. Stickney

### Graduate Students

P. C. Abbott  
M. Balooch

R. H. Habert

T. E. Kenney  
D. E. Mathes

### RESEARCH OBJECTIVES AND SUMMARY OF RESEARCH

The general purpose of our research program is to study problems relating to the atomic, molecular, and electronic processes occurring at gas-solid interfaces. Examples of these processes are: thermionic emission, surface ionization, adsorption, absorption, oxidation, catalysis by metals, electrode processes in electrical discharges, and the scattering of molecular beams from solid surfaces. Such processes are encountered in thermionic energy converters, electron tubes, ion propulsion engines, lamps, high-speed flight, and high-temperature nuclear reactors. At present, we are concentrating on the following problems.

#### 1. Desorption of Hydrogen from Metals

We have measured the spatial distribution and speed distribution of hydrogen molecules desorbed from the surfaces of polycrystalline and single-crystal nickel samples at temperatures ranging from 500° to 1000°C. The results show that the desorbed molecules do not have the expected Maxwellian distribution; instead, they are concentrated along the surface normal and their mean energy is ~45% greater than that of an equilibrium gas at the temperature of the solid. By using Auger electron spectroscopy, we have shown that surface impurities (e. g., S and C) are responsible for the unexpected distributions. Similar results have been obtained for other metals (Fe, Pt, Nb, and stainless steel). Only in the case of copper does the effect persist when the surface is cleaned, and we now plan to study copper in more detail by using single crystals. We believe that these experimental techniques provide a unique source of data that will prove to be valuable in the development of more accurate models of various gas-solid rate processes, including catalytic recombination, desorption, and sublimation.

#### 2. Kinetics of Vaporization Processes

The sublimation of graphite has received a great deal of attention recently because of its importance in various high-temperature applications. Results obtained in different laboratories do not agree well, most probably because the evaporation coefficients of the molecular species ( $C_2, C_3, C_4$ ) depend strongly upon the structure of the graphite surface. We believe that the apparatus developed for our desorption studies (described above) provides a unique method for obtaining detailed information on the kinetics of vaporization processes, and we shall measure the spatial and speed distributions of carbon molecules as they evaporate from graphite crystals of different structures. We also are planning similar measurements of other materials which are reported to have very low evaporation coefficients (e. g., As, P, S). The results of our recent measurements of arsenic sublimation are described in Section IX-A. We

---

\*This work was supported principally by the Joint Services Electronics Programs (U. S. Army, U. S. Navy, and U. S. Air Force) under Contract DAAB07-71-C-0300, and in part by the National Aeronautics and Space Administration (Grant NGR 22-009-091).

## (IX. PHYSICAL ELECTRONICS AND SURFACE PHYSICS)

shall use the data to test existing models of vaporization and/or to develop an improved model. Our results may also provide a clearer understanding of the reverse process, i. e., the condensation, nucleation, and growth of a solid by vapor deposition.

### 3. Auger Electron Spectrometer for Determining the Chemical Composition of Surfaces at High Temperature

We have demonstrated that Auger electron spectroscopy (AES) may be utilized over a far greater range of temperature than the present accepted range. As a specific illustration, we have employed AES to determine the amount of oxygen adsorbed on a polycrystalline tungsten specimen at temperatures from 300° to 2400° K. We shall perform similar studies using single crystals, which will enable us to determine the dependence of oxygen adsorption on surface structure. With this extension of the useful range of AES, the technique may now be used to great advantage in studies of high-temperature surface processes (e. g., oxidation, corrosion, catalysis, and impurity segregation).

### 4. High-Temperature Gas-Solid Chemical Reactions

A factor limiting many high-temperature engineering devices and systems is the high rate of attack of refractory materials by the reactive components of the gaseous environment. We have developed a simple theoretical model that predicts the rate of attack for a specific gas-solid system if we have sufficient information on (a)  $\Delta G_i$ , the free energies of formation of the dominant volatile species, and (b)  $\zeta$ , the equilibration probability. This probability is the fraction of the impinging gas molecules that attains chemical equilibrium with the solid rather than being scattered (reflected) without being equilibrated. Satisfactory agreement has been obtained for two gas-solid systems (O-W and O-Mo), but we are unable to provide predictions for other gas-solid systems because of insufficient data on  $\Delta G_i$  and  $\zeta$ . Therefore, we propose to obtain the necessary data on  $\Delta G_i$  and  $\zeta$  for several systems that are of practical importance (e. g., systems involving oxygen, halogens, and refractory metals). Molecular beam techniques and Auger electron spectroscopy will be utilized in these experiments.

### 5. Diffraction of Helium Atoms from a Tungsten Crystal

We believe that we have made the first observation of the diffraction of atoms by a clean metal surface. Since diffraction was observed from the (112) face of tungsten but not for the (110) face, it appears that diffraction depends strongly upon the three-dimensional atomic structure of the surface rather than only on the two-dimensional periodicity of the surface structure.

### 6. Other Studies

(a) We plan to use Auger electron spectroscopy and mass spectrometry to investigate the reaction of oxygen and nitrogen with SiC and SiN, which are two of the materials currently being considered for the stator blades of gas turbines. (b) We shall extend our studies of adsorption, permeation, and desorption processes to include metals that are expected to be used in controlled thermonuclear (fusion) reactors. (c) We propose to investigate the influence of impurities on the weldability and the high-temperature creep behavior of W and Mo. Data obtained in our laboratory and elsewhere indicate that both the weldability and the creep behavior are influenced markedly by bubbles formed in the material as a result of certain volatile impurities. Our goal will be to determine methods for controlling the bubbles to obtain the desired properties.

R. E. Stickney

A. MEASUREMENTS OF THE SPEED AND SPATIAL DISTRIBUTIONS  
OF ARSENIC MOLECULES EVAPORATED FROM AN  
As(111) CRYSTAL

The kinetics of vaporization of solids and liquids has been studied in considerable detail<sup>1-5</sup> because, as well as being an interesting fundamental problem, the kinetics is influential in certain technological processes involving either vaporization or the reverse process, condensation. Particular attention has been given to materials that exhibit "retarded vaporization," that is, the measured rate of vaporization of the material into vacuum is lower than the rate predicted on the basis of equilibrium kinetic theory using the equilibrium vapor pressure and the assumption that the vaporization coefficient is unity. Since retarded vaporization is observed for materials that vaporize primarily as molecules rather than as atoms, it is suspected that the rate-limiting step may be the formation of molecules at preferred sites on the surface. Various models of this step have been proposed, and there have been discussions of the possibility that the evaporated molecules may have excess translational energy<sup>6</sup> and/or a nondiffuse spatial distribution.<sup>7</sup> To test this suggestion, we have measured the speed and spatial distributions of arsenic molecules evaporated from an arsenic crystal. Arsenic is a classic example of retarded vaporization, and existing data<sup>1</sup> show that As is the dominant vapor species at the temperatures considered here (310-345°C).

In a previous investigation in our laboratory<sup>8</sup> we measured the speed and spatial distributions of hydrogen molecules desorbed from a nickel surface. Results indicated that the desorbed molecules have excess translational energy and are concentrated in the vicinity of the surface normal. We decided, therefore, to determine whether similar results obtain in the case of vaporization of a pure material. We used our laboratory's "speed distribution apparatus," which has been described in detail elsewhere,<sup>8</sup> but we employed an As crystal in place of the Ni membrane. The crystal was grown by a modified Bridgman technique, and was cleaved in air at 77°K to expose the (111) face. We mounted the crystal disk, 8 mm in diameter and 3 mm thick, in a manner that allowed us to vary the angular position of the surface relative to the detector, thereby enabling us to measure both the spatial and speed distributions with the same apparatus. The crystal was heated from the rear by radiation from a hot filament, and its temperature was determined by a thermocouple attached to the crystal support (a stainless-steel assembly heated to the same temperature as the crystal).

The time-of-flight (TOF) technique used to determine the speed distribution of the evaporated  $\text{As}_4$  molecules has been described elsewhere.<sup>8</sup> The TOF curve shown in Fig. IX-1 is for the conditions  $T = 345^\circ\text{C}$  and  $\theta = 0^\circ$ , where  $T$  is the crystal temperature, and  $\theta$  is the angle of inspection relative to the surface normal. The stepped curve is the output signal from a multichannel signal-averaging instrument, and the filled

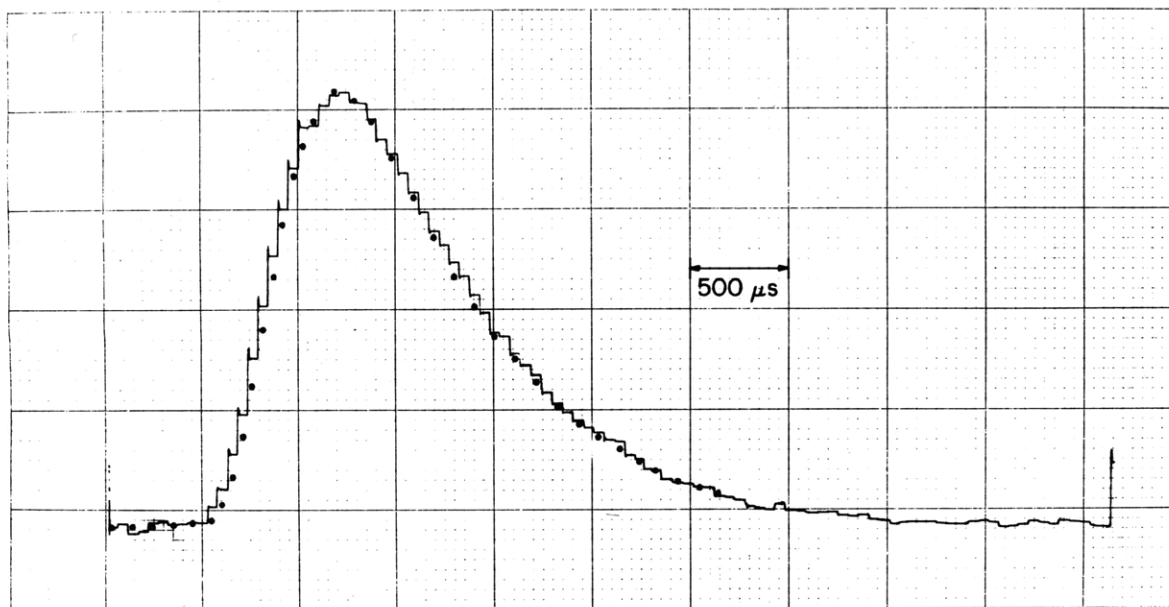


Fig. IX-1. Time-of-flight data for molecules evaporated from an As(111) crystal at 345°C. Stepped curve: experimental data (the output signal from a multichannel signal-averaging instrument). Filled circles: calculations (for an equilibrium gas of  $\text{As}_4$  molecules having a Maxwellian speed distribution with temperature equal to that of the crystal).

circles represent the TOF curve calculated for an equilibrium gas of  $\text{As}_4$  molecules having a Maxwellian speed distribution with temperature equal to that of the crystal.<sup>8,9</sup> Although the amplitude of the Maxwellian TOF curve has been normalized to fit the maximum of the experimental curve, no adjustments were made to force the maxima to occur at the same point on the time scale. The agreement between the curves is sufficiently close to suggest that the speed distribution of the evaporated molecules is Maxwellian with the same temperature as the crystal. Similar measurements were performed at other values of  $T$  and  $\theta$ , and the results are in agreement with the corresponding Maxwellian distribution within the accuracy of the technique.

For the spatial distribution measurements the detector was changed from a density-sensitive (through-flow) gauge to a flux-sensitive (stagnation) gauge by totally enclosing the ionization region with solid walls except for the entrance aperture for the molecular beam and the aperture through which the ions are extracted and accelerated into an electron multiplier. (The sticking probability on the walls for  $\text{As}_4$  appeared to be sufficiently low that the "pumping" of molecules by condensation on the walls was small.) A lock-in amplifier was used in place of the signal-averaging instrument to improve the output signal-to-noise ratio. Since there is a small collimating aperture (2mm diam) between the crystal and the detector, the area of the crystal surface inspected ("seen")

by the detector varies as  $(\cos \theta)^{-1}$ . Therefore, to obtain the spatial distribution per unit surface area, the detector signal was multiplied by  $\cos \theta$ . The experimental data presented in Fig. IX-2 indicate that the spatial distribution is diffuse. (The deviation

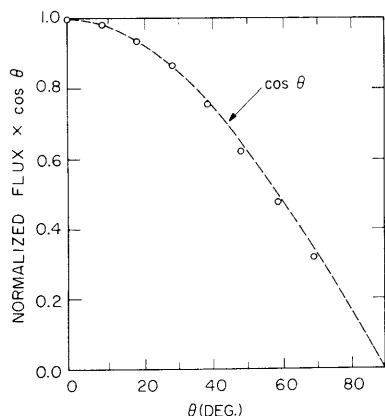


Fig. IX-2.

Experimental measurement of the spatial distribution of arsenic molecules evaporated from an As(111) crystal at 310°C.

observed for  $\theta \geq 50^\circ$  is to be expected because the area seen by the detector is no longer proportional to  $(\cos \theta)^{-1}$  when  $\theta$  is sufficiently large that the detector "sees" the edge of the crystal.) Similar results were observed for other temperatures and crystals.

After completing the experimental measurements, the crystal surface was inspected by scanning electron microscopy and found to be faceted as described by previous investigators.<sup>1</sup> Therefore, our results correspond to a complicated average of the properties present on the faceted surface of molecules evaporating from a variety of crystallographic sites (e.g., ledges, kinks, and terraces).

The present results indicate that  $\text{As}_4$  molecules evaporated from an As(111) crystal have a diffuse spatial distribution and a Maxwellian speed distribution with the temperature equal to that of the crystal. That is, the molecules appear to be completely equilibrated to the crystal in the sense that their spatial and speed distributions have the same forms (but not the same absolute magnitudes) as those of the equilibrium vapor that would exist above the crystal in an ideal Knudsen cell. We conclude that the excess activation energy of  $\sim 9$  kcal/mole observed<sup>10</sup> for the sublimation of As(111) does not lead to a detectable excess translational energy of the evaporated molecules.

These results should be useful in guiding the development of theoretical models of the vaporization process of arsenic. For example, Brumbach and Rosenblatt<sup>11</sup> have utilized our results to estimate several bounds on the parameters appearing in their model.

M. Balooch, A. E. Dabiri, R. E. Stickney

(IX. PHYSICAL ELECTRONICS AND SURFACE PHYSICS)

References

1. G. M. Rosenblatt, in G. R. Belton and W. L. Worrell (Eds.), Heterogeneous Kinetics at Elevated Temperature, (Plenum Press, New York, 1970), p. 209.
2. A. W. Searcy, in A. W. Searcy, D. W. Ragone, and V. Colombo (Eds.), Chemical and Metallurgical Behavior of Inorganic Materials (Interscience Publishers, Inc., New York, 1970), p. 107.
3. G. A. Somorjai and J. E. Lester, *Progr. Solid State Chem.* 4, 1 (1967).
4. J. P. Hirth and G. M. Pound, "Condensation and Evaporation," *Progr. Materials Sci.* 11, 1-190 (1963).
5. O. Knacke and I. N. Stranski, *Progr. Metal Phys.* 6, 181 (1956).
6. For example, see R. W. Mar and A. W. Searcy, *J. Chem. Phys.* 49, 182 (1968).
7. For example, see the discussion in J. P. Hirth and G. M. Pound, *op. cit.*, pp. 8-12.
8. A. E. Dabiri, T. J. Lee, and R. E. Stickney, *Surface Sci.* 26, 522 (1971).
9. T. E. Kenney, A. E. Dabiri, and R. E. Stickney, *Quarterly Progress Report No. 102*, Research Laboratory of Electronics, M.I.T., July 15, 1971, p. 39.
10. G. M. Rosenblatt and P. K. Lee, *J. Chem. Phys.* 49, 2995 (1968).
11. S. B. Brumbach and G. M. Rosenblatt, Private communication.

B. EFFECT OF OXYGEN ADSORPTION ON THE SCATTERING OF HELIUM AND ARGON ATOMS FROM A W(112) CRYSTAL

1. Introduction

In fundamental studies of the interaction of gases with solid surfaces, we usually attempt to work with a surface that is well defined, that is, with one that is clean, smooth, and monocrystalline. It is known, however, that it is extremely difficult to remove surface impurities from some materials,<sup>1</sup> and that facets are thermodynamically stable on surfaces of certain crystallographic orientations.<sup>2</sup> Moreover, in some cases it is these impurities or facets that are responsible for the technological importance of a material. For these reasons, we planned to study the influence of surface impurities and facets on the nature of the interaction of gas atoms with solid surfaces.

In this experimental study molecular-beam techniques are used to study the scattering of He and Ar from a W(112) single crystal. The effect of oxygen adsorption on the scattering of He and Ar is studied by obtaining scattering data for different surface conditions including clean surfaces and surfaces having different oxygen coverages. With helium and argon, the interaction can be simplified because the particles are both monoatomic and inert. Also, helium might be expected to be particularly sensitive to atomic-scale surface roughness because of its small diameter and weak interaction potential. We have selected tungsten as a solid surface because its surface properties and cleaning processes have been studied in detail, and there is a vast literature on the

adsorption and faceting properties of different crystal faces of tungsten.<sup>3-6</sup> Specifically, the (112) face of tungsten was selected because it has a highly anisotropic structure

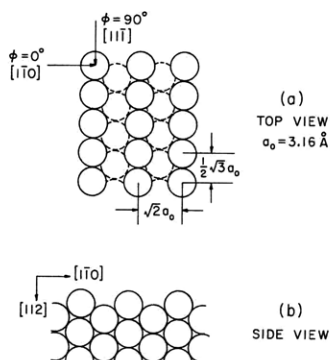


Fig. IX-3.

Atomic structure of the (112) face of a tungsten single crystal.

containing closely packed rows of top-layer atoms in the  $[11\bar{1}]$  direction separated by relatively open channels or troughs (see Fig. IX-3).

The reason for choosing oxygen as the adsorbate is that, aside from carbon, oxygen appears to be the most tenacious contaminant of tungsten, and therefore interferes with the use of the other adsorbates. Also, detailed LEED data<sup>4, 5</sup> are available on the adsorption of oxygen on the (112) face of tungsten. As indicated by LEED data,<sup>4</sup> the (112) face of tungsten when heated in oxygen develops (110) facets having an average width of 3-5 tungsten atoms. Facets of this

size are too small to be observed clearly by electron microscopy, but we hope that they can be detected by measuring the helium scattering pattern. An attempt has been made to observe the effect of faceting on the helium scattering pattern.

## 2. Experimental Apparatus and Procedures

The experimental apparatus is identical to that described previously<sup>7</sup> except that the target chamber is now pumped by an ion pump and the detector is a stagnation-type ionization gauge (details have been reported elsewhere<sup>8</sup>). The target chamber pressure is of the order of  $1 \times 10^{-9}$  Torr after baking at  $200^\circ\text{C}$ . A nearly monoenergetic molecular beam, generated by a nozzle source, strikes the target situated at the center of the target chamber. Detection of either the incident beam or the scattered beam in the principal scattering plane is accomplished by the rotatable detector.

The tungsten target is a disk, oriented and spark-cut from a high-purity single crystal such that the surface is the (112) face. Before mounting, the crystal surface was polished, first mechanically and then electrolytically, and the orientation was checked by the Laue x-ray diffraction technique. After installing the crystal in the apparatus and baking the system during evacuation, the surface was cleaned. Specifically, the carbon impurities were removed by the oxidation procedure described by Germer and May<sup>6</sup> (that is, a repeated cycle of heating the crystal at  $\sim 1300^\circ\text{K}$  in  $\sim 2 \times 10^{-7}$  Torr  $\text{O}_2$  for a considerable time and then flashing for a few seconds above  $2400^\circ\text{K}$ ). Also, before measuring a scattering pattern, the crystal was flashed to remove adsorbable background gases. Unfortunately, the background pressure ( $\sim 1 \times 10^{-9}$  Torr

## (IX. PHYSICAL ELECTRONICS AND SURFACE PHYSICS)

with beam off) proved to be too high to maintain the surface clean for the time required to measure a scattering pattern unless  $T_s \geq 1200^\circ\text{K}$ . Hence we could not obtain reliable scattering patterns for  $T_s$  below  $\sim 1300^\circ\text{K}$  (this point is discussed in detail elsewhere<sup>7</sup>).

### 3. Experimental Results

#### a. Clean Surface

Since our measurements of the scattering of helium from a clean W(112) surface have been reported previously,<sup>8</sup> we shall concentrate here on similar measurements performed for argon. Figure IX-4 shows the scattering patterns for 3 values of  $\theta_i$ , the angle of incidence of the argon beam (measured from the surface normal). The average energy of the beam atoms,  $E_i$ , was  $\sim 0.06$  eV, and the temperature of the crystal,  $T_s$ , was  $2200^\circ\text{K}$ . The azimuthal orientation was such that the beam was parallel to the

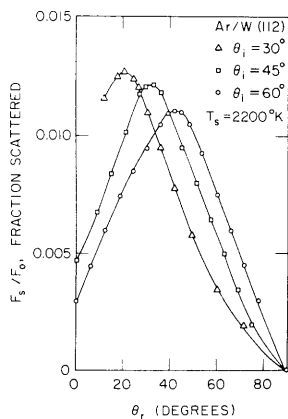


Fig. IX-4.

Scattering patterns for Ar scattered from a W(112) crystal. Beam conditions:  $E_i \approx 0.06$  eV,  $\Phi = 0^\circ$ ,  $\theta_i = 30^\circ$ ,  $45^\circ$ , and  $60^\circ$ . Target conditions:  $T_s \approx 2200^\circ\text{K}$ .

$[1\bar{1}0]$  direction of the surface lattice (see Fig. IX-3). Similar data were obtained, however, when the beam was parallel to the  $[1\bar{1}\bar{1}]$  direction, thereby indicating that the nature of the Ar-W(112) scattering process does not depend strongly on the azimuthal direction.

#### b. Oxygen-Covered Surface

To study the effect of oxygen adsorption on the scattering patterns, the following procedures were used to obtain different oxygen coverages.

(i)  $O_i$  procedure: The crystal was flashed to  $2200^\circ\text{K}$  to remove adsorbed gases and then cooled to room temperature in oxygen at  $2 \times 10^{-7}$  Torr. The purpose of this procedure was to ensure that the surface was covered primarily with adsorbed oxygen; however, it is realized that the surface was contaminated to some degree by adsorption of other constituents of the residual gas, mainly CO. The oxygen was then pumped out, the beam turned on, and scattering data were obtained for increasing temperatures of the crystal.



(IX. PHYSICAL ELECTRONICS AND SURFACE PHYSICS)

(ii)  $O_c$  procedure: This procedure is similar to (i), except that the oxygen pressure,  $p_{O_2}$ , was maintained at  $\sim 5 \times 10^{-8}$  Torr or, in some cases, changed to desired values in the range from  $2 \times 10^{-9}$  to  $5 \times 10^{-7}$  Torr. Scattering data were then obtained for various values of  $T_s$  after allowing sufficient time for the oxygen coverage to reach a steady-state value in each case. Since coverage at a given temperature increases with increasing  $p_{O_2}$ , this procedure enables us to observe the dependence of the scattering pattern on oxygen coverage at a constant temperature.

In all cases the results were obtained for the same angle of incidence,  $\theta_i = 60^\circ$ . For each gas the angular position of the detector,  $\theta'_r$ , was chosen to equal the position of the peak of the scattering pattern for the particular gas scattered from the clean (112) crystal at  $T_s = 2200^\circ\text{K}$ ; that is,  $\theta'_r = \theta_i$  for helium and  $\theta'_r = 42^\circ$  for argon at  $\theta_i = 60^\circ$ . The data illustrate the dependence of the peak intensity on temperature for different procedures, the temperature being increased in steps.

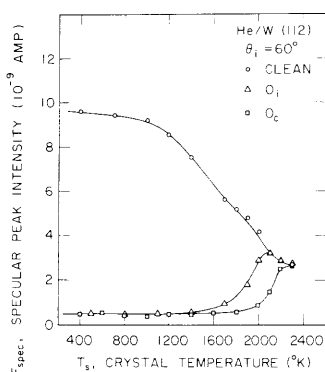


Fig. IX-5.

Dependence of specular peak intensity on crystal temperature,  $T_s$ , for He scattered from W(112) for oxygen coverages corresponding to the  $O_i$  and  $O_c$  procedures.

The data corresponding to the  $O_i$  procedures are shown in Figs. IX-5 and IX-6 for helium and argon beams, respectively. At lower temperatures oxygen adsorption causes the scattering intensity to be very small because the scattering patterns are nearly diffuse. Notice that the scattering intensity remains almost constant in the temperature range 300-1500°K. As the temperature is increased above 1500°K, the intensity increases because the patterns are changing from diffuse to lobular. At  $T_s > 2100^\circ\text{K}$ , the patterns are the same as those for the "clean" surface, which indicates that the oxygen coverage becomes negligibly small above 2100°K with the  $O_i$  procedure.

Figures IX-5 and IX-6 also show the data corresponding to the  $O_c$  procedure with  $p_{O_2} \approx 5 \times 10^{-8}$  Torr. In this case also the intensities are much smaller at lower temperatures, but they are independent of temperature for a larger range, 300-~1900°K. Above 1900°K the intensities increase with temperature and the  $O_c$  curve joins the "clean" and the  $O_i$  curves at  $T_s \approx 2300^\circ\text{K}$ .

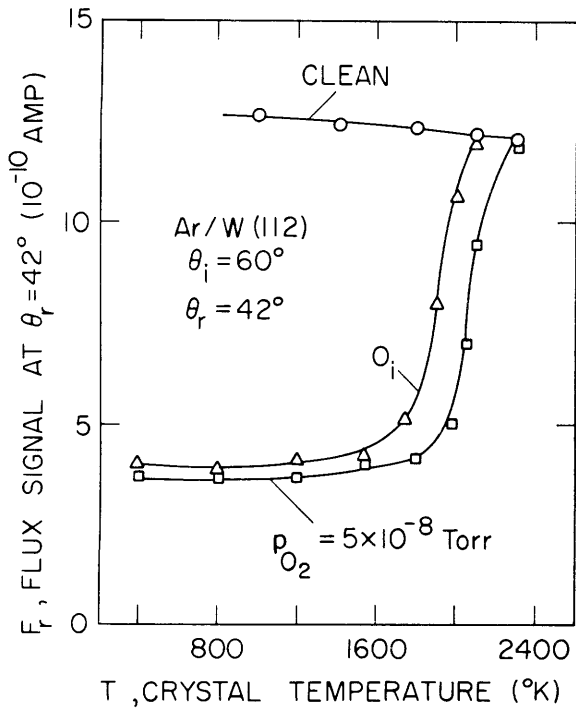


Fig. IX-6.  
Dependence of scattering intensity on  $T_s$  for Ar scattered from W(112) for oxygen coverages corresponding to the  $O_i$  and  $O_c$  procedures.

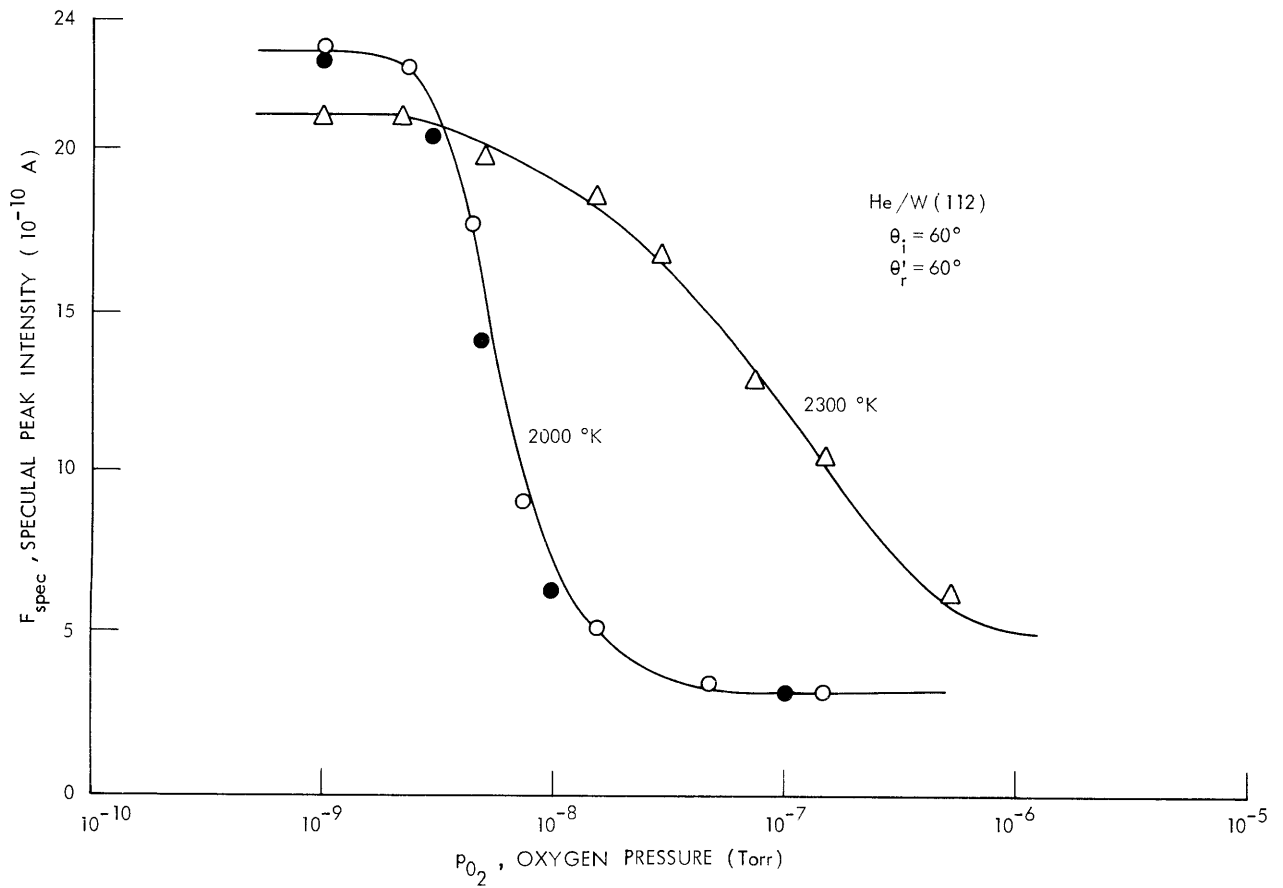


Fig. IX-7. Scattering isotherms for He scattered from W(112).

(IX. PHYSICAL ELECTRONICS AND SURFACE PHYSICS)

Figure IX-7 shows the dependence of the helium scattering peak intensity on the oxygen pressure for two values of the crystal temperature, 2000°K and 2300°K. As can be seen, the peak intensity decreases rapidly as the oxygen pressure is increased above  $1 \times 10^{-9}$  Torr, and it reaches a minimum at  $p_{O_2} \approx 5 \times 10^{-8}$  Torr at  $T_s = 2000^\circ\text{K}$ . The filled circles represent data taken subsequently by decreasing the pressure in steps, and the agreement with the data for increasing pressure indicates that adsorption is reversible for these values of temperature and pressure. At lower temperatures, we observed that adsorption was not reversible.

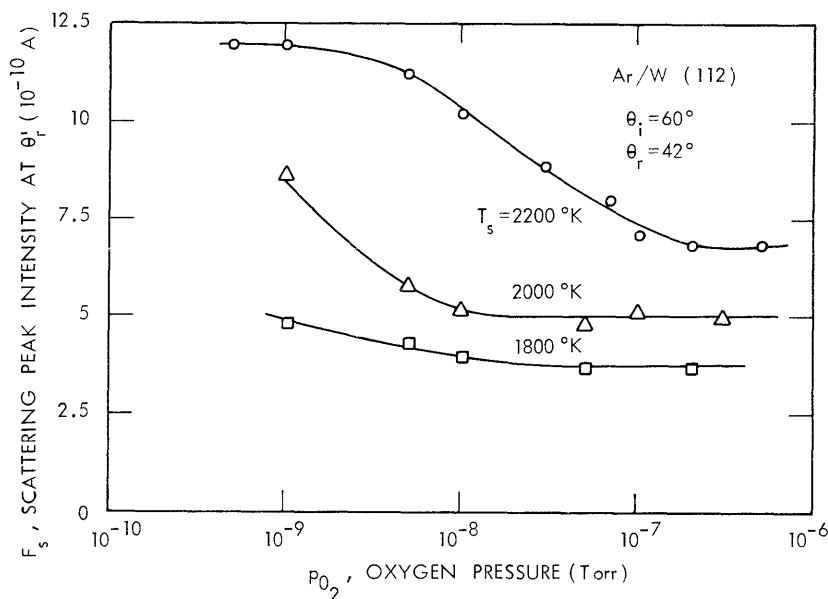


Fig. IX-8. Scattering isotherms for Ar scattered from W(112).

Similar data for argon are presented in Fig. IX-8, and the general behavior is essentially the same as in the case of helium.

c. Faceted Surface

According to the existing LEED data,<sup>4,5</sup> exposure of the (112) face of tungsten to oxygen while it is held between 1300°K to 1700°K produces a regular array of (110) microfacets covered with a layer of oxygen atoms. The size of the facets increases with the oxygen exposure. The surface structure which has been suggested as an explanation of the  $p(1 \times 3)$  LEED pattern for the faceted surface is shown in Fig. IX-9, and we point out that it exposes strips of (101) and (011) planes that are only 3 atoms wide.<sup>4</sup> As can be seen from Fig. IX-9, these facet planes are inclined at 30° with respect to the original (112) plane. At an exposure of  $\sim 200$  L (one L =  $1 \times 10^{-6}$  Torr-s), a well-formed

## (IX. PHYSICAL ELECTRONICS AND SURFACE PHYSICS)

(1×5) pattern is observed having facet planes 5 atoms wide.

In the present experiment the crystal was held at 1500°K and was exposed to  $5 \times 10^{-8}$  Torr  $O_2$  for ~70 minutes, giving a total exposure of ~210 L. According to the LEED data,<sup>4</sup> with this exposure facets having the (1×5) pattern are formed. As mentioned

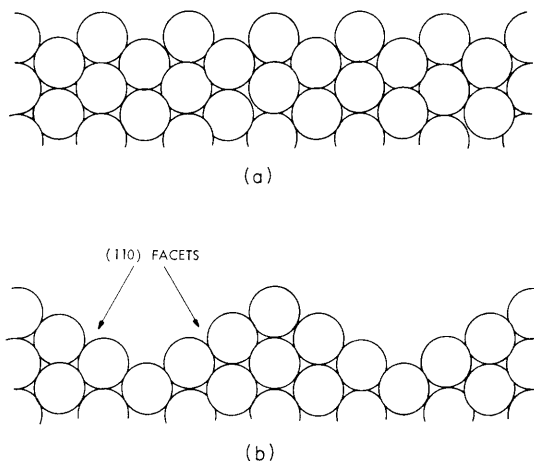


Fig. IX-9.

Illustration of the (110) facets that form on a W(112) crystal surface as a result of heating the crystal in oxygen. (a) Ideal (112) surface. (b) Faceted (112) surface.

above, these facet planes are inclined at  $30^\circ$  to the (112) plane. Hence, if helium scatters pseudospecularly from these facet planes, we can estimate the angular positions of the scattering peaks from simple geometry. Accordingly, the incident angle  $\theta_i$  can be selected in such a way that we can observe the maximum effect of faceting on the scattering patterns. Unfortunately, the facet planes face each other at  $120^\circ$  and therefore the specular reflections from these planes for any angle of incidence  $\theta_i$  are such that it is impossible for the detector to reach both the angular positions of the specular reflections, because of the geometrical limitation on the detector rotation. Taking this fact into account, an attempt was made to observe only one peak, if present, corresponding to different angles of incidence  $\theta_i$  in the range  $0-60^\circ$ .

The He scattering patterns from the faceted surface were nearly diffuse, similar to those for  $O_i$  and  $O_c$  procedures, with very small intensities. We did not observe any peak corresponding to specular reflection from the facet plane. The crystal temperature was then increased in steps and the specular peak ( $\theta_r = \theta_i$ ) intensities were measured. This curve was similar to the one corresponding to the  $O_i$  procedure in Fig. IX-5.

### 4. Results

A discussion of the present results, including a comparison of the results for W(112) with those obtained previously<sup>7</sup> for W(110), has appeared elsewhere.<sup>9</sup> In that discussion we have also attempted to relate our scattering data to existing

(IX. PHYSICAL ELECTRONICS AND SURFACE PHYSICS)

data on the nature of the adsorption of oxygen on (112) and (110) tungsten crystals.

D. V. Tendulkar, R. E. Stickney

References

1. R. W. Roberts, Brit. J. Appl. Phys. 14, 537 (1963).
2. A. J. W. Moore, in Metal Surfaces: Structure, Energetics, and Kinetics (American Society for Metals, Metals Park, Ohio, 1963), pp. 155-198.
3. See the recent review by G. Ehrlich, in Annual Reviews of Physical Chemistry (Annual Reviews, Inc., Palo Alto, Cal., 1966), Vol. 17, pp. 295-322; forty-one references on tungsten are listed in A. G. Jackson et al., "A Bibliography on Low Energy Electron Diffraction and Related Techniques," Report ARL69-0003, Aerospace Research Laboratory, Wright-Patterson Air Force Base, Ohio, January 1969.
4. C. C. Chang and L. H. Germer, Surface Sci. 8, 115 (1967); C. C. Chang, Ph.D. Thesis, Cornell University, September 1967; published as Material Science Center Report No. 720, Cornell University, Ithaca, New York.
5. J. C. Tracy and J. M. Blakely, Surface Sci. 13, 313 (1968); J. C. Tracy, Ph.D. Thesis, Cornell University, September 1968; published as Material Science Center Report No. 1017, Cornell University, Ithaca, New York.
6. L. H. Germer and J. W. May, Surface Sci. 4, 452 (1966).
7. S. Yamamoto and R. E. Stickney, J. Chem. Phys. 53, 1594 (1970).
8. D. V. Tendulkar and R. E. Stickney (to appear in Surface Sci.); see also Quarterly Progress Report No. 102, Research Laboratory of Electronics, M.I.T., July 15, 1971, pp. 33-49.
9. R. E. Stickney, D. V. Tendulkar, and S. Yamamoto (to appear in J. Vac. Sci. Technol.).

